*Proc. Natl. Acad. Sci. USA*
Vol. 95, pp. 14147–14151, November 1998
Biophysics

# NMR scalar couplings across Watson–Crick base pair hydrogen bonds in DNA observed by transverse relaxation-optimized spectroscopy

KONSTANTIN PERVUSHIN*, AKIRA ONO†, CÉSAR FERNÁNDEZ*, THOMAS SZYPERSKI*, MASATSUNE KAINOSHO†, AND KURT WÜTHRICH*‡

*Institut für Molekularbiologie und Biophysik, Eidgenössische Technische Hochschule, Hönggerberg CH-8093 Zürich, Switzerland; and †Department of Chemistry, Faculty of Science, Tokyo Metropolitan University, 1–1 Minamiohsawa, Hachioji 192-0397, Japan

*Contributed by Kurt Wüthrich, September 23, 1998*

**ABSTRACT** **This paper describes the NMR observation of $^{15}N$—$^{15}N$ and $^{1}H$—$^{15}N$ scalar couplings across the hydrogen bonds in Watson–Crick base pairs in a DNA duplex, $^{h}J_{NN}$ and $^{h}J_{HN}$. These couplings represent new parameters of interest for both structural studies of DNA and theoretical investigations into the nature of the hydrogen bonds. Two dimensional [$^{15}N$,$^{1}H$]-transverse relaxation-optimized spectroscopy (TROSY) with a $^{15}N$-labeled 14-mer DNA duplex was used to measure $^{h}J_{NN}$, which is in the range 6–7 Hz, and the two-dimensional $^{h}J_{NN}$-correlation-[$^{15}N$,$^{1}H$]-TROSY experiment was used to correlate the chemical shifts of pairs of hydrogen bond-related $^{15}N$ spins and to observe, for the first time, $^{h}J_{HN}$ scalar couplings, with values in the range 2–3.6 Hz. TROSY-based studies of scalar couplings across hydrogen bonds should be applicable for large molecular sizes, including protein-bound nucleic acids.**

Hydrogen bonds in biological macromolecules can usually only be inferred, rather than directly evidenced by experimental techniques (1), including NMR spectroscopy (2). Here we describe the observation by two-dimensional (2D) [$^{15}N$,$^{1}H$]-transverse relaxation-optimized spectroscopy (TROSY) (3–5) of scalar couplings across the Watson–Crick base pairs in isotope-labeled DNA, which affords direct observation of the hydrogen bonds in these structures. Scalar couplings across hydrogen bonds have been previously reported for organic-synthetic compounds (6, 7), RNA fragments (8), and a metalloprotein (9, 10). The variability of such couplings observed so far indicates that they may become sensitive new parameters for detection of hydrogen bond formation and associated subtle conformational changes. Furthermore, in conjunction with quantum-chemical calculations, precise measurements of scalar couplings across hydrogen bonds can be expected to provide novel insights into the nature of hydrogen bonds in chemicals and in biological macromolecules.

## MATERIALS AND METHODS

Fully and partially $^{13}C$,$^{15}N$-doubly labeled DNA oligomers were synthesized on a DNA synthesizer (Applied Biosystems model 392–28) by the solid-phase phosphoroamidite method, by using isotope-labeled monomer units that had been synthesized according to a previously described strategy (11). Approximately 1 $\mu$mol of oligomer was obtained from 5 $\mu$mol of nucleoside bound to the resin. NMR samples of the DNA duplex at a concentration of ≈2 mM were prepared in 90% $H_2O$/10% $D_2O$ containing 50 mM potassium phosphate and 20 mM KCl at pH 6.0. NMR measurements were performed at 15°C on Bruker DRX500 and DRX750 spectrometers equipped with $^{1}H$-{$^{13}C$,$^{15}N$} triple-resonance probeheads.

For the present study, an estimate of the line widths to be expected from the use of TROSY was of critical interest. To estimate the reduction of the $^{15}N$ and $^{1}H$ relaxation rates in TROSY when compared with conventional spectroscopy, one needs information on the principal values and orientations of the chemical shift tensors of $^{15}N$ and $^{1}H$, as well as on the $^{15}N$—$^{1}H$ distance (3–5). Here, we collected this information from the following sources: An estimate of the chemical shift anisotropy tensor of the imino $^{15}N$ spin was obtained by use of the solid-state NMR data (12) on $^{15}N_3$ in uracil, which has principal values of $\delta_{11}$ = 200 ppm, $\delta_{22}$ = 131 ppm, and $\delta_{33}$ = 79 ppm, with the largest component oriented at 9° relative to the $^{15}N_3$–$^{1}H_3$ bond and the smallest component perpendicular to the ring plane. For the imino proton, we used $\Delta\sigma$ = 8 ppm, based on the measured anisotropy, $\Delta\sigma = \delta_{11} - 0.5(\delta_{22} + \delta_{33})$, of ≈6 ppm in 2′,3′,5′-tri-*O*-benzoyl(3-$^{15}N$)uridine (13) and the available data on hydrogen-bonded amino protons (14–18). For the imino $^{15}N$—$^{1}H$ bond length, the solid-state NMR value of 0.11 nm for G and T in a hydrated DNA duplex (19) was used. Relaxation of the imino proton due to dipole–dipole (DD) coupling with remote protons in the DNA duplex was represented as follows (2): in the Watson–Crick A═T pair by an adenosine amino proton at a distance of 0.24 nm and the adenosine C2 proton at 0.3 nm; in G≡C by a guanosine amino proton at 0.22 nm and a cytosine amino proton at 0.25 nm. For both base pairs, two imino protons in sequentially stacked bases at 0.4 nm also were considered. Following the calculations outlined in refs. 3–5, the use of TROSY at a polarizing magnetic field $B_o$ = 17.6 T is expected to yield 65% and 30% reductions of the $^{15}N$ and $^{1}H$ linewidth, respectively, for A═T base pairs and 55% and 20% reductions for G≡C base pairs. If the contributions from dipolar interactions with remote protons are neglected, the calculations predict reductions of 85% and 75% for $^{15}N$ and $^{1}H$ in both A═T and G≡C base pairs, which may perhaps be in part exploited when working with $H_2O/D_2O$ mixed solvents.

## RESULTS AND DISCUSSION

The theoretical considerations presented in the preceding section predict that compared with the corresponding conventional NMR experiments, [$^{15}N$,$^{1}H$]-TROSY (3–5) yields ≈70% and 30% reductions of the $^{15}N$ and $^{1}H$ linewidths, respectively, when used to record signals for the guanosine $^{15}N_1$—$^{1}H_1$ and thymidine $^{15}N_3$—$^{1}H_3$ imino groups in a $^{15}N$-labeled DNA duplex. The reduced TROSY line widths then allow direct measurements of $^{15}N$—$^{15}N$ and $^{1}H$—$^{15}N$ scalar spin–spin

The publication costs of this article were defrayed in part by page charge payment. This article must therefore be hereby marked "*advertisement*" in accordance with 18 U.S.C. §1734 solely to indicate this fact.



Abbreviations: TROSY, transverse relaxation-optimized spectroscopy; E.COSY, exclusive correlation spectroscopy; DD, dipole–dipole coupling; 2D, two-dimensional.

‡To whom reprint requests should be addressed. Institute für Molekularbiologie und Biophysik, Eidgenössische Technische Hochschule Hönggerberg, CH-8093 Zürich, Switzerland.

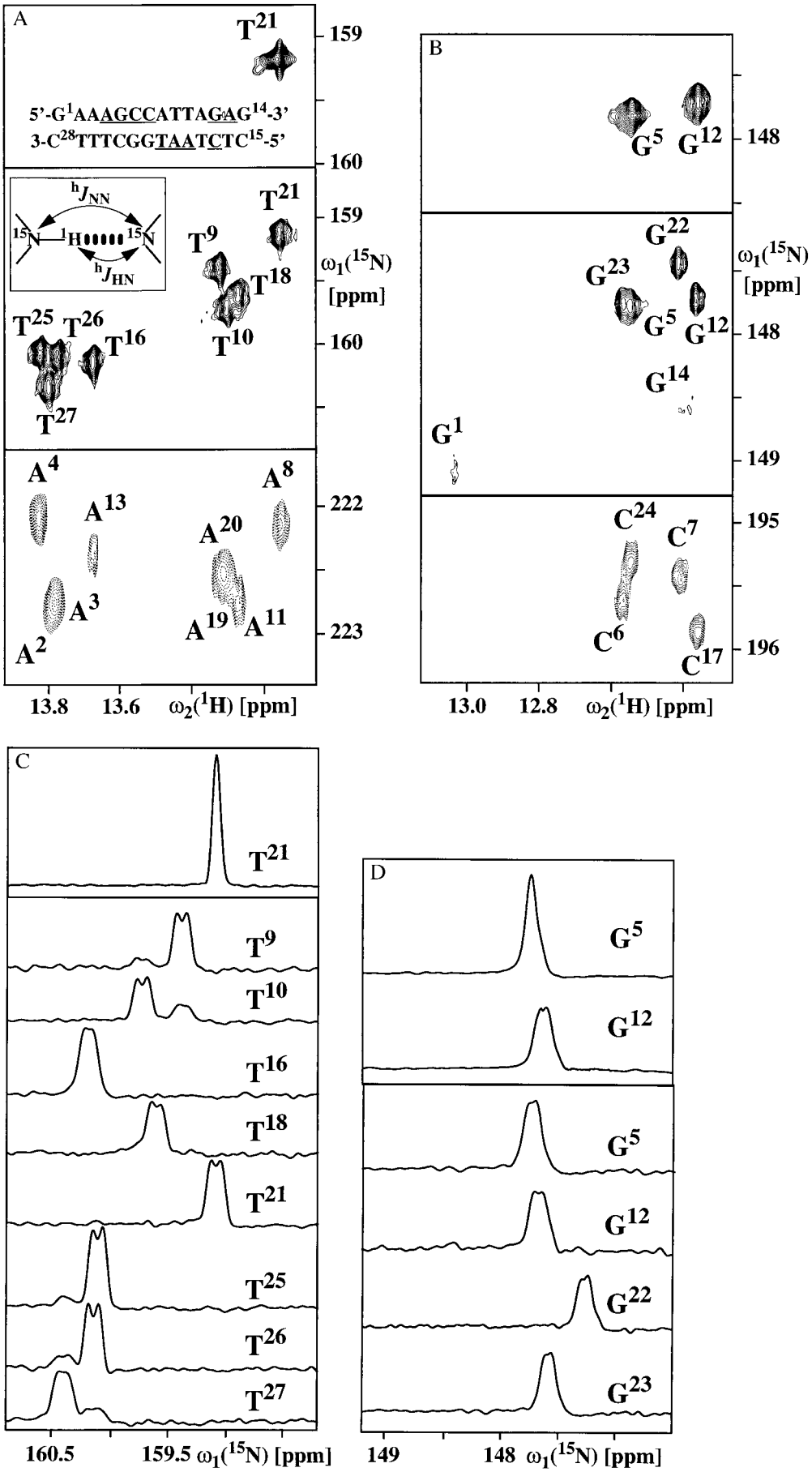


FIG. 1. (*Legend appears at the bottom of the opposite page.*)

couplings across hydrogen bonds, $^{h}J_{NN}$ and $^{h}J_{HN}$, respectively. Fig. 1 *A* and *B*, shows regions of the 2D [$^{15}$N,$^{1}$H]-TROSY spectra measured with two differently $^{15}$N-labeled 14-bp DNA duplexes. For the uniformly $^{15}$N-labeled duplex, an in-phase splitting along $\omega_1(^{15}N)$ is observed for all imino $^{15}$N spins involved in Watson–Crick base pairs (Fig. 1*C*). A first indication that these splittings are due to spin–spin coupling came from the observation that the measured $^{h}J_{NN}$ values are independent of the strength of the polarizing magnetic field, $B_o$, as evidenced by experiments at $^{1}$H frequencies of 500 and 750 MHz. To unambiguously identify the origin of this splitting, an identical spectrum was recorded for a partially $^{15}$N-labeled duplex, in which either only one or both nucleotides in the individual Watson–Crick base pairs are $^{15}$N-labeled (20, 21). For example, the [$^{15}N_1$,$^{1}H_1$]-correlation peak of G$^{12}$ shows a doublet fine structure, whereas the cross-peak of G$^{5}$ appears as a singlet, since C$^{24}$ is not $^{15}$N-labeled (Fig. 1*D Upper*). Similarly, T$^{21}$ shows doublet and singlet fine structures, respectively, in the two differently labeled duplexes (Fig. 1*C*), confirming that the splitting observed in the uniformly labeled duplex is due to $^{15}$N—$^{15}$N coupling.

In addition to the observation of the resolved in-phase splittings in the 2D [$^{15}$N,$^{1}$H]- TROSY spectra (Fig. 1 *C* and *D*), precise values for $^{h}J_{NN}$ were obtained by inverse Fourier transformation of the in-phase multiplets (22). Table 1 shows that there are sizeable variations in the $^{h}J_{NN}$ couplings among the A═T base pairs, e.g., T$^{10}$ and T$^{16}$ (Fig. 1*C*), as well as among the G≡C base pairs (Fig. 1*D*), which probably reflect local differences in Watson–Crick base pairing geometry and/or dynamic processes such as fraying of the chain ends.

The new 2D $^{h}J_{NN}$-correlation-[$^{15}$N,$^{1}$H]-TROSY experiment (Fig. 2) uses the slowly relaxing component of the imino $^{15}$N doublet to relay magnetization via $^{h}J_{NN}$ across the hydrogen bond to the tertiary $^{15}$N position of the second base in the Watson–Crick base pair. The sensitivity of the experiment is further enhanced by use of both the $^{1}$H and $^{15}$N steady–state magnetizations (3–5, 23). The correlation of the chemical shifts of pairs of hydrogen bond-related nucleotides should be of particular interest for unambiguous identification of base pairs in DNA or RNA molecules exhibiting a distinct tertiary structure. The inherent high sensitivity of [$^{15}$N,$^{1}$H]-TROSY for studies of large molecular sizes (3–5) should enable the use of this approach with large nucleic acid fragments, and with nucleic acids in protein complexes.

The coupling constants $^{h}J_{NN}$ appear to be smaller for G≡C than for A═T base pairs (Fig. 1 *C* and *D*), which possibly reflects the longer $^{15}$N—$^{15}$N distance in G≡C when compared with A═T base pairs (1, 8). In principle, the $^{h}J_{NN}$ values could be estimated from the ratio of the direct and relayed cross-peak volumes (Fig. 1), provided that the $^{15}$N—$^{15}$N antiphase magnetization does not relax much faster than $^{15}$N in-phase magnetization (24–26). However, even for small nucleic acid fragments with rotational correlation times of ≈10 ns, 2D [$^{15}$N,$^{1}$H]-TROSY provides an ≈fivefold improved sensitivity when compared with 2D $^{h}J_{NN}$-correlation-[$^{15}$N,$^{1}$H]-TROSY (Fig. 2), so that it is preferable to use inverse Fourier transformation of the in-phase peaks in 2D [$^{15}$N,$^{1}$H]-TROSY to determine the $^{h}J_{NN}$ couplings (22).

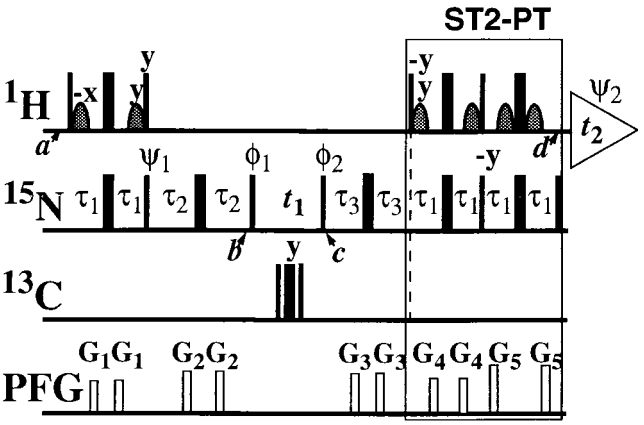


FIG. 2. Experimental scheme for the 2D $^{h}J_{NN}$-correlation-[$^{15}$N,$^{1}$H]-TROSY experiment used to correlate the chemical shifts of pairs of hydrogen bond-related $^{15}$N spins and to measure $^{h}J_{HN}$. On the lines marked $^{1}$H, $^{15}$N, and $^{13}$C, narrow and wide bars stand for nonselective 90° and 180° radio frequency pulses, respectively, with the carrier frequencies at 12, 190, and 145 ppm, respectively. The delays are $\tau_1$ = 2.7 ms, $\tau_2$ = 18 ms, and $\tau_3 = \tau_2 - \tau_1$. The line marked PFG indicates the pulsed magnetic field gradients applied along the *z* axis: $G_1$, amplitude 30 G/cm, duration 1 ms; $G_2$, 42 G/cm, 1 ms; $G_3$, 45 G/cm, 1 ms; $G_4$, 40 G/cm, 1 ms; and $G_5$, 48 G/cm, 1 ms. Two data sets, I and II, are measured in the interleaved manner with the following phase cycling schemes: (I), $\phi_1$ = {−x, x}; $\phi_2$ = {2(−x),2x}; $\psi_1$ = {4y,4(−y)}; $\psi_2$(receiver) = {y,−y,−y,y,−y,y,y,−y}; (II), $\phi_1$ = {−y,y}; $\phi_2$ = {2(−y),2y}; $\psi_1$ = {4(−x),4x}; $\psi_2$(receiver) = {−x, x,x,−x, x,−x,−x, x}; x on all other pulses. For both data sets, quadrature detection in the $t_1$ dimension is obtained by using States-TPPI (38) by simultaneously incrementing each of the phases $\phi_2$ and $\psi_2$ by 90°. The transfer of $^{15}$N magnetization to $^{1}$H for detection of single transition-to-single transition polarization transfer (5) was used. Fourier transformation of the sum and difference of the two data sets results in two 2D $^{h}J_{NN}$- correlation-[$^{15}$N,$^{1}$H]-TROSY spectra in which the relative cross-peak positions are determined in E.COSY manner by the chemical shifts and the scalar-coupling constants (27–30). For example, both the direct and the relayed correlation cross-peaks that appear in the two spectra are shifted by $^{1}J_{HN}$ along $\omega_2(^{1}H)$. Along $\omega_1(^{15}N)$, the direct peaks also are shifted by $^{1}J_{HN}$, but the separation of the relayed cross-peaks is determined exclusively by $^{h}J_{HN}$. To enhance the signals of rapidly exchanging imino protons, water saturation is minimized by keeping the water magnetization along +z during the entire experiment, using the water-selective 90° pulses indicated by curved shapes on the line $^{1}$H.

When the TROSY-type detection scheme ST2-PT (5) was combined with exclusive correlation spectroscopy (E.COSY) (27–30), the 2D $^{h}J_{NN}$-correlation-[$^{15}$N,$^{1}$H]-TROSY experiment of Fig. 2 allowed, for the first time, observation and quantification of $^{h}J_{HN}$ couplings between tertiary $^{15}$N atoms and the imino proton across the Watson–Crick hydrogen bond in DNA (Fig. 3). In the E.COSY patterns for covalently linked $^{15}$N—$^{1}$H moieties and the hydrogen-bonded $^{15}$N. . . $^{1}$H combinations (Fig. 3), a positive sign of $^{h}J_{HN}$ can be inferred from the negative sign of $^{1}J_{HN}$ (31). A significantly larger relative variation is observed for the $^{h}J_{HN}$ couplings in the individual base pairs than for $^{h}J_{NN}$, with values ranging from 2 Hz to 3.6 Hz (Table 1). Notably, there is a significant correlation

FIG. 1. (*On the opposite page.*) NMR observation of scalar $^{15}$N—$^{15}$N couplings across hydrogen bonds in DNA, $^{h}J_{NN}$. (*A Top and Middle*) Contour plots of the region containing signals of A═T base pairs from [$^{15}$N,$^{1}$H]-TROSY spectra (3, 5) of the partially and uniformly $^{13}$C,$^{15}$N-labeled DNA duplex, respectively. (*A Bottom*) Contour plot showing the relayed cross-peaks obtained with 2D $^{h}J_{NN}$-correlation-[$^{15}$N,$^{1}$H]-TROSY, where the broken contours indicate negative spectral intensities. The direct [$^{15}N_3$(T),$^{1}H_3$(T)]-correlations (*Top and Middle*) and the relayed [$^{15}N_1$(A),$^{1}H_3$(T)] cross-peaks (*Bottom*) of the A═T base pairs are shown. Chemical shifts are relative to 2,2-dimethyl-2-silapentane-5-sulfonate sodium salt (DSS). The DNA sequence is shown in the *Top*, where the $^{15}$N- and $^{13}$C-containing nucleotides in the partially $^{13}$C,$^{15}$N-labeled DNA (see text) are underlined. (*Insert*) Definition of the scalar couplings $^{h}J_{NN}$ and $^{h}J_{HN}$ in Watson–Crick base pairs. (*B*) Same presentation as *A* for the G≡C base pairs. (*C*) Cross sections along $\omega_1(^{15}N)$ through the individual cross peaks in the spectra (*A*). (*C Lower*) Direct correlation cross-peaks in the uniformly $^{13}$C,$^{15}$N-labeled DNA duplex. (*C Upper*) Direct correlation cross peaks in the partially labeled duplex. (*D*) Same presentation as *C* for cross sections along $\omega_1(^{15}N)$ taken through the individual cross peaks in the spectra (*B*).

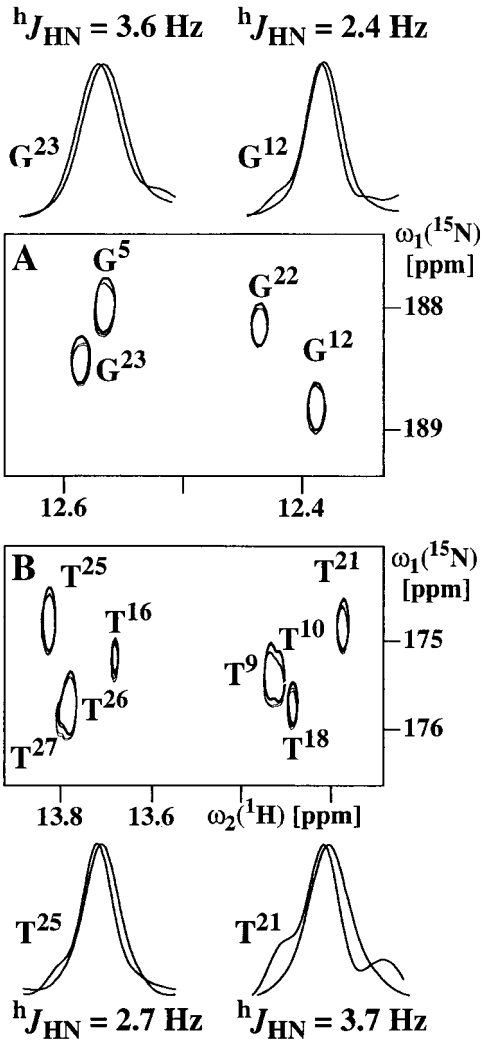


FIG. 3. NMR observation of scalar $^1H$—$^{15}N$ couplings across hydrogen bonds in DNA, $^hJ_{HN}$. The plots show comparisons of the sum and difference 2D $^hJ_{NN}$-correlation-[$^{15}N$,$^1H$]-TROSY spectra recorded with the uniformly $^{13}C$,$^{15}N$-labeled DNA duplex (Fig. 1*A*) on a Bruker DRX-750 spectrometer, using the experimental scheme of Fig. 2. (*A* and *B*) Contour plots with signals from G≡C base pairs and A═T base pairs, respectively. To facilitate comparison, one spectrum was shifted relative to the other by ≈90 Hz along $\omega_2$($^1$H), so that corresponding peaks overlap along this dimension. The relayed cross-peaks from each of the two spectra are represented by two contour lines. For selected base pairs, superpositions of cross sections along $\omega_1$($^{15}$N) taken through the original, unshifted peaks are shown above and below the two panels, where the two peaks to be compared have been normalized to the same intensity. The shift between the two peaks provides an E.COSY-type representation of $^hJ_{HN}$ (see text).

between the magnitudes of corresponding $^hJ_{HN}$ and $^hJ_{NN}$ couplings within each type of nucleotides (Table 1), with the only exceptions of $G^5$ and $T^{16}$.

The nature of the $^hJ_{HN}$ and $^hJ_{NN}$ interactions as scalar couplings due to electron-coupled interactions between the related nuclear spins (32) is clearly evidenced: (*i*) the observed in-phase splittings (Fig. 1) are field-independent; and (*ii*) the observed relative magnitudes of corresponding $^hJ_{HN}$ and $^hJ_{NN}$ pairs could not be explained by residual DD coupling (33–35). It has been suggested that the Fermi-contact term, which usually dominates scalar couplings through covalent bonds (32), is also effective for scalar couplings through hydrogen bonds (36, 37). Since both the donor imino group and the acceptor nitrogen are embedded in $\pi$-conjugated systems, $\pi$-bond polarization upon "cyclic" hydrogen bond formation could give rise to $\pi$-cooperativity and thus enhance the hydrogen bond stability and the covalent character of the hydrogen bonds (1). In fact, this view seems to be supported by measurements of scalar $^hJ_{HH}$ couplings of 1–2 Hz between hydroxyl and formyl protons in O-*H*... O═C*H* moieties attached to $\pi$-conjugated 1,6-dioxapyrene derivatives, where the $^hJ_{HH}$ couplings could only be observed in the presence of a substituent that donates additional $\pi$-bond polarization (6).

Table 1. Values and SDs of $^{15}N$—$^{15}N$ and $^1H$—$^{15}N$ scalar spin–spin couplings across hydrogen bonds, $^hJ_{NN}$ and $^hJ_{HN}$, in Watson–Crick base pairs in DNA (see Fig. 1A).

| Residue | $^hJ_{NN}$, Hz | $^hJ_{HN}$, Hz |
|---|---|---|
| $T^9$ | 6.7 ± 0.1 | 3.6 ± 0.1 |
| $T^{10}$ | 7.0 ± 0.1 | 3.2 ± 0.3 |
| $T^{16}$ | 6.5 ± 0.1 | 2.0 ± 0.2 |
| $T^{18}$ | 6.8 ± 0.1 | 2.7 ± 0.2 |
| $T^{21}$ | 6.5 ± 0.1 | 3.7 ± 0.3 |
| $T^{25}$ | 7.0 ± 0.1 | 2.7 ± 0.2 |
| $T^{26}$ | 6.9 ± 0.1 | 2.7 ± 0.1 |
| $T^{27}$ | 7.0 ± 0.1 | 1.8 ± 0.2 |
| $G^5$ | 6.0 ± 0.1 | 2.8 ± 0.3 |
| $G^{12}$ | 6.3 ± 0.1 | 2.4 ± 0.5 |
| $G^{22}$ | 6.5 ± 0.1 | 2.9 ± 0.6 |
| $G^{23}$ | 6.4 ± 0.1 | 3.6 ± 0.5 |

We thank Dr. S. Grzesiek for informing us about similar work with RNA in his laboratory before ref. 8 appeared in print. Financial support by the Schweizerischer Nationalfonds (project 31.49047.96) and by Core Research Evolutional Science and Technology (CREST) of the Japan Science and Technology Corporation (J.S.) is gratefully acknowledged.

1. Jeffrey, G. A. & Saenger, W. (1991) *Hydrogen Bonding in Biological Structures* (Springer, Berlin).
2. Wüthrich, K. (1986) *NMR of Proteins and Nucleic Acids* (Wiley, New York).
3. Pervushin, K., Riek, R., Wider, G. & Wüthrich, K. (1997) *Proc. Natl. Acad. Sci. USA* **94,** 12366–12371.
4. Pervushin, K., Riek, R., Wider, G. & Wüthrich, K. (1998) *J. Am. Chem. Soc.* **120,** 6394–6400.
5. Pervushin, K., Wider, G. & Wüthrich, K. (1998) *J. Biomol. NMR* **12,** 345–348.
6. Platzer, N., Buisson, J. P. & Demerseman, P. (1992) *J. Heterocyclic. Chem.* **29,** 1149–1153.
7. Shenderovich, A., Smirnov, S. N., Denisov, G. S., Grindin, V. A., Golubev, N. S., Dunger, A., Kirpekar, S., Malkina, O. L. & Limbach, H.-H. (1998) *Ber. Bunsenges. Phys. Chem.* **102,** 422–428.
8. Dingley, A. J. & Grzesiek, S. (1998) *J. Am. Chem. Soc.* **120,** 8293–8297.
9. Blake, P. R., Park, J. B., Adams, M. W. W. & Summers, M. F. (1992) *J. Am. Chem. Soc.* **114,** 4931–4933.
10. Blake, P. R., Lee, B., Summers, M. F., Adams, M. W. W., Park, J. B., Zhou, Z. H. & Bax, A. (1992) *J. Biomol. NMR* **2,** 527–533.
11. Ono, A., Tate, S. & Kainosho, M. (1994) in *Stable Isotope Applications in Biomolecular Structure and Mechanisms*, eds. Trewhella, J., Cross, T. A. & Unkefer, C. J. (Los Alamos National Laboratory, Los Alamos, NM), pp. 127–144.
12. Anderson-Altmann, K. L., Phung, C. G., Mavromoustakos, S., Zheng, Z., Facelli, J. C., Poulter, D. & Grant, D. M. (1995) *J. Phys. Chem.* **99,** 10454–10458.
13. Guéron, M., Leroy, J. L. & Griffey, R. H. (1983) *J. Am. Chem. Soc.* **105,** 7262–7266.
14. Michal, C. A., Wehman, J. C. & Jelinski, L. W. (1996) *J. Magn. Reson. B* **111,** 31–39.
15. Ramamoorthy, A., Wu, C. H. & Opella, S. J. (1997) *J. Am. Chem. Soc.* **119,** 10479–10486.
16. Gerald, R., II, Bernhard, T., Haeberlen, U., Rendell, J. & Opella, S. J. (1993) *J. Am. Chem. Soc.* **115,** 777–782.
17. Tjandra, N. & Bax, A. (1997) *J. Am. Chem. Soc.* **119,** 8076–8082.
18. Tessari, M., Vis, H., Boelens, R. & Kaptein, R. & Vuister, G. (1997) *J. Am. Chem. Soc.* **119,** 8985–8990.

19. DiVerdi, J. A. & Opella, S. J. (1982) *J. Am. Chem. Soc.* **104,** 1761–1762.
20. Szyperski, T., Ono, A., Fernández, C., Kainosho, M. & Wüthrich, K. (1998) *J. Am. Chem. Soc.* **120,** 821–822.
21. Fernández, C., Szyperski, T., Ono, A., Iwai, H., Tate, S., Kainosho, M. & Wüthrich, K. (1998) *J. Biomol. NMR* **12,** 25–37.
22. Szyperski, T., Güntert, P., Otting, G. & Wüthrich, K. (1992) *J. Magn. Reson.* **99,** 552–560.
23. Szyperski, T., Braun, D., Banecki, B. & Wüthrich, K. (1996) *J. Am. Chem. Soc.* **118,** 8146–8147.
24. Bax, A., Max, D. & Zax, D. (1992) *J. Am. Chem. Soc.* **114,** 6923–6924.
25. Bax, A., Vuister, G. W., Grzesiek, S., Delaglio, F., Wang, A. C., Tschudin, R. & Zhu, G. (1994) *Methods Enzymol.* **239,** 79–105.
26. Grzesiek, S., Vuister, G. W. & Bax, A. (1993) *J. Biomol. NMR* **3,** 487–493.
27. Schwalbe, H., Rexroth, A., Eggenberger, T., Geppert, T. & Griesinger, C. (1993) *J. Am. Chem. Soc.* **115,** 7878–7879.
28. Hu, J. S. & Bax, A. (1997) *J. Am. Chem. Soc.* **119,** 6360–6368.
29. Montelione, G. T. & Wagner, G. (1989) *J. Am. Chem. Soc.* **111,** 5474–5475.
30. Griesinger, C., Sørensen, O. W. & Ernst, R. R. (1987) *J. Magn. Reson.* **75,** 474–492.
31. Bystrov, V. F. (1976) *Prog. NMR Spectrosc.* **10,** 41–81.
32. Kowalewski, J. (1977) *Prog. NMR Spectrosc.* **11,** 1–78.
33. Kung, H. C., Wang, K. Y., Goljer, I. & Bolton, P. H. (1995) *J. Magn. Reson. B* **109,** 323–325.
34. Tolman, J. R., Flanagan, J. M., Kennedy, M. A. & Prestegard, J. H. (1995) *Proc. Natl. Acad. Sci. USA* **92,** 9279–9283.
35. Tjandra, N. & Bax, A. (1997) *Science* **278,** 1111–1114.
36. Xia, B., Wilkens, S., Westler, W. M. & Markley, J. L. (1998) *J. Am. Chem. Soc.* **120,** 4893–4894.
37. Wilkens, S., Xia, B., Weinhold, F., Markley, J. L. & Westler, W. M. (1998) *J. Am. Chem. Soc.* **120,** 4806–4814.
38. Marion, D., Ikura, M., Tschudin, R. & Bax, A. (1989) *J. Magn. Reson.* **39,** 163–168.